Research Square

Preprints are preliminary reports that have not undergone peer review.
They should not be considered conclusive, used to inform clinical practice,
or referenced by the media as validated information.

Multi-quality optimization of turn-milling AISI 52100 hollow cylindrical rods using weighted index integration

Hua Huang
Wuhan University of Technology
Li-jia Chen
Wuhan University of Technology
Chi-Chen Liu
Lunghwa University of Science and Technology
Chi-Hsuan Hsieh
Lunghwa University of Science and Technology
Chung-Chen Tsao
aetcc@mail.lhu.edu.tw
Lunghwa University of Science and Technology
Chun-Yao Hsu
Lunghwa University of Science and Technology

Research Article

Keywords: Turn-milling machining, Desirability function analysis, Multi-quality optimization technique

Posted Date: November 13th, 2026

DOI: https://doi.org/10.21203/rs.3.rs-11553151/v1

License: This work is licensed under a Creative Commons Attribution 4.0 International License.
Read Full License

Multi-quality optimization of turn-milling AISI 52100 hollow cylindrical rods using weighted index integration

Hua Huang[1,2], Li-jia Chen[1], Chi-Chen Liu[3], Chi-Hsuan Hsieh[3], Chung‑Chen Tsao[3]*, Chun-Yao Hsu[3]*

[1]School of Navigation, Wuhan University of Technology, Wuhan 430063, China

[2]School of Marine Engineering, Zhejiang International Maritime College, Zhoushan 316021, China

[3]Department of Mechanical Engineering, Lunghwa University of Science and Technology, Taoyuan 33306, Taiwan

Abstract

Power tool holders (PTHs) play a crucial role in turn-milling machining (TMM); however, the cantilever effect reduces the selection of process parameters for workpiece milling. AISI 52100 is a high-carbon chromium bearing steel with a surface hardness of HRC 63 after heat treatment, exhibiting excellent wear resistance and strength. Nevertheless, it also presents challenges such as high cutting load, rapid tool wear, and difficulty in controlling surface quality. Multi-quality optimization technologies (MQOTs) have been successfully applied to many advanced industrial machining processes. Therefore, this study investigates the MQOTs of AISI 52100 hollow cylindrical rods (HCRs) in TMM. A 6 mm tungsten carbide end mill was used to mill a groove with a depth of 1.5 mm and a width of 10 mm, and four TMM parameters were systematically modified: cutting speed (A), feed rate (B), depth of cut (C), and cooling method (D). By combining MQOTs (DFA and GRA) with entropy weight method (EWM), multiple quality characteristics can be transformed into a single quality characteristic, while minimizing roundness error (RE) and surface roughness (SR), and maximizing tool life (TL) and material removal rate (MRR). The optimal TMM parameters were determined through analysis of variation (ANOVA) to be $A_3B_2C_1D_2$ (cutting speed 100 m/min, feed rate 0.06 mm/rev, depth of cut 0.10 mm, emulsified oil cooling). These parameters were validated experimentally, resulting in an increase in TL from 27 pieces to 33 pieces, an increase in MRR from 26.14 mm^3/s to 30.40 mm^3/s, a decrease in RE from 0.010 mm to 0.009 mm, and a decrease in SR from 0.238 μm to

0.218 μm. This study demonstrates that combining multiple quality optimization strategies (DFA and GRA) with EWM effectively overcomes the difficult-to-machine characteristics of AISI 52100 and addresses the machining efficiency and quality of PTHs in TMM.

Keywords: Turn-milling machining, Desirability function analysis, Multi-quality optimization technique.

*Correspondence author. Fax: +886 2 82094845.

E-mail: aetcc@mail.lhu.edu.tw (C.-C. Tsao), cyhsu@mail.lhu.edu.tw (C.-Y. Hsu)

1. **Introduction**

Turn-milling compound machines (TMCMs) are a type of digital machine tool that combines the functions of traditional lathes and milling machines. They can complete multiple machining processes (such as turning, milling, drilling, tapping or grinding) on a single machine, thus greatly improving the efficiency and precision of the increasingly numerous component processing in various industries such as automobiles, aerospace, and defense. Compared with traditional machine tools, TMCMs have significant differences in mechanical structure and machining operation methods [1].

The power tool holder (PTH) is a cantilever structure extending from the turret of a machining center, thus inherently limiting its rigidity, speed, and torque. Currently, the two mainstream interface standards for connecting the PTH to the turret are Base Mount Turret (BMT) and Verein Deutscher Ingenieure (VDI). Because the overhang length of the PTH is much greater than that of the machining center spindle, vibration or chatter when machining on a shared cutting surface, thus affecting the machined

surface quality of the entire workpiece [2]. Typically, the speed of the PTH is only 1/3 to 1/2 of that of the machining center spindle, and the high speed results in low torque [3]. For difficult-to-machine materials (such as titanium alloys and Inconel), the low speed of the PTH becomes a bottleneck in machining. Therefore, the PTH of a TMCM is not suitable for heavy cutting or large-area face milling. Although the rigidity of the BMT interface is better than that of VDI, it still cannot compare with that of a dedicated milling machine spindle.

Many scholars have previously studied the characteristics of TMM. Karaguzel et al. [4] found that tool axis offset can improve cutting forces, surface quality and tool life (TL) in TMM operations. Liao et al. [5] confirmed that studying cutting layer (CL) geometry and the change of cutting forces (CFs) contributes to the formation of chips and changes in cutting temperature, force and chatter of TMM, thereby improving the quality and efficiency of machining and the TL. Since the tool sweep area of TMM is related to tool wear, Cai et al. [6] optimized the sweep area with processing parameters (cutting depth, cutting angle, eccentricity and processing length), and the optimized processing parameters can reduce tool wear and increase TMM TL. Zhu et al. [7] studied the influence of machining parameters (cutting speed of cutter, cutting speed of workpiece, axial feed velocity and eccentric) on chip length and thickness in TMM of Al-6061. In addition, they also established a mathematical model based on the trajectory function and proposed the machining parameter selection criteria for TMM qualitatively and quantitatively. Ning and Zhu [8] investigated the effects of the number of teeth, tool speed, feed rate and tool radius on the surface morphology of the workpiece. They found that as the tool speed increased, it was beneficial to improve the surface quality. Therefore, TMM of the AISI 52100 bearing steel without compromising the groove plane integrities has remained a competitive challenge for researcher and

manufacturing engineers.

The optimization of processing parameters not only ensures processing quality, but also achieves higher productivity. However, single-quality optimization technology (SQOT) as an assessment may not be reliable when dealing with key parameter selections that directly impact process acceptability. Therefore, multi-quality optimization technologies (MQOTs) are found to be useful tools for systematically handling key parameter selection problems involving multiple conflicting qualities or objectives. The MQOTs have been widely applied in engineering design, manufacturing, management and other various fields. Weighted index integration (DFA, GRA, TOPSIS) and heuristic algorithms (GA, NSGA-II, PSO) are commonly used to solve MQOT problems. Compared to heuristic algorithms, weighted index integration is faster, more intuitive, and more suitable for engineering optimization scenarios with limited experimental data and high experimental costs. DFA and GRA are widely employed to address multi-quality optimization problems. Both methods integrate multiple quality characteristics of a product into a single comprehensive index, thereby enabling the identification of optimal parameter combinations. They are particularly well suited for product and process optimization, encompassing planning, experimental implementation, result evaluation, and determination of the optimal levels of control factors [9-14]. Jin and Fang [15] conducted high-speed TMM experiments on aluminum alloy using machining parameters (tool speed, axial feed, and feed per tooth). They confirmed through analysis of variation (ANOVA) that tool speed is an important factor affecting surface roughness (SR). Ekici et al. [16] applied GRA to evaluate the effects of cutting speed, feed rate, and tool treatments on milling Ti6AI4V alloy. Research shows that as the cutting speed increases, the cutting force decreases, but the SR of the workpiece increases. Increasing the feed rate significantly increases the

cutting force, and the SR first decreases and then increases. The optimal cutting parameters are determined through GRA of the responses. Sghaier et al. [17] used GRA and principal component analysis (PCA) to evaluate the effects of depth of cut, feed rate, cutting speed, and lubrication method (dry lubrication and micro-lubrication) on SR, cutting force, and MRR during laser powder bed melt forming of 17-4PH stainless steel. Their results showed that feed rate primarily affects SR, while depth of cut controls cutting force and overall machining performance. Compared to geometric parameters, minimum quantity lubrication (MQL) has a limited impact, mainly contributing to improved cutting stability and surface integrity. Jattakul et al. [18] compared the DFA and the genetic algorithm (GA) under selected solid-state copper brazing conditions (brazing temperature, holding time and loading pressure) to find the optimum brazing conditions of maximum brazed-joint tensile shear force. The experimental results show that the brazed-joint tensile shear force is significantly affected by all three brazing parameters. The optimal brazing conditions are brazing temperature of 620°C, holding time of 30min, and load pressure of 12.173 kPa. And the optimal brazing conditions predicted by the DFA and GA are actually the same. Cardoso et al. [19] used response surface method and DFA-based optimization technology to study the multi-objective quality (SR and MRR) of turning duplex stainless steel UNS S32760. They found that the optimal processing conditions for minimizing SR and maximizing MRR were set as cutting depth (ap) = 1.34 mm, feed rate (f) = 0.16 mm/rev., and cutting speed (Vc) = 186.81 m/min.

AISI 52100 bearing steel has good fatigue resistance and wear resistance and has received increasing attention. The hardness exceeds 700 HV, the tensile strength is in the range of 1570~1960 MPa, and the fracture toughness K_{Ic} is in the range of 14~18 MPa $m^{1/2}$ [20]. It is suitable for various mechanical parts such as bearings, molds, guide

rails, and rollers. RE is the geometrical property of a cross-section intended to be circular, and out-of-roundness in cylindrical parts can significantly impact assembly accuracy [21].

Since TMM technology has the advantages of both turning and milling, it has attracted more and more attention from related processing industry operators. However, the TMM's PTH cantilever structure has inherent limitations in rigidity, speed, and torque, making it difficult to set optimal cutting parameters for multi-quality characteristics (MQCs). In order to achieve this goal, this study summarizes the use of the optimal technology (DFA and GRA) to determine the optimal multi-quality process parameter combination through the TMM AISI 52100 HCRs data of tungsten carbide end mill. Finally, the multi-quality optimal parameter combination of AISI 52100 HCRs for TMM processing was verified through confirmation experiments. The MQOT proposed in this study provides effective guidance for efficient machining strategies for TMM.

2. **Optimization technology**

Optimization technique is a method to find the optimal state of a system or model under specific conditions. When faced with the problem of conflicting MQCs, choices and compromises are required. Since optimizing TMM AISI 52100 bearing steel is a manufacturing problem with MQCs considered, the optimization technology is very suitable for practical application in manufacturing processes.

2.1 entropy-weight method (EWM)

Weighting is a very effective way to evaluate when different processes or factors have different proportions or varying degrees of importance in the overall process.

Therefore, weights are widely used in engineering, business management, investment, neural networks and other various fields. Because the EWM is objective, simple and universal, it is often used to evaluate the importance of MQCs indicators. The steps for calculating entropy-weight are as follows [22-24].

Step 1: Developed data matrix (X). The assessment data for the MQCs is used to represent the degree to which each alternative *i* exerts a direct effect on each attribute *j* (x_{ij}).

$$X_{ij} = \begin{bmatrix} x_{11} & x_{12} & \cdots & x_{1n} \\ x_{21} & x_{22} & \cdots & x_{2n} \\ \vdots & \vdots & \ddots & \vdots \\ x_{m1} & x_{m2} & \cdots & x_{mn} \end{bmatrix} (i = 1,2...,m; j = 1,2...,n) \quad (1)$$

Step 2: Normalized data matrix (r_{ij}). The maximum and minimum quality characteristics for each attribute are respectively normalized using Eq. (2) and Eq. (3):

$$r_{ij} = \frac{X_{ij} - \min(X_{ij})}{\max(X_{ij}) - \min(X_{ij})} \ (i = 1,2...,m; j = 1,2...,n) \quad (2)$$

$$r_{ij} = \frac{\max(X_{ij}) - X_{ij}}{\max(X_{ij}) - \min(X_{ij})} \ (i = 1,2...,m; j = 1,2...,n) \quad (3)$$

Step 3: Calculate the entropy of each attribute with a value between 0 and 1.

$$e_j = -\frac{\sum_{i=1}^{m} f_{ij} \ln(f_{ij})}{\ln(m)} \ (i = 1,2...,m; j = 1,2...,n) \quad (4)$$

where $f_{ij} = \frac{r_{ij}}{\sum_{i=1}^{m} r_{ij}}$ is the probability of occurrence. If f_{ij} are all the same, the entropy values for each attribute have a maximum value $(e_j = 1)$. If f_{ij} is 0, then $f_{ij} \ln(f_{ij})$ is 0.

Step 4: Calculated entropy weights (w_j) .

$$w_j = \frac{1 - e_j}{n - \sum_{i=1}^{m} e_j} \ (j = 1,2...,n) \tag{5}$$

where $\sum_{j=1}^{n} w_j = 1$, $(1 - e_j)$ is the dispersion intensity for each attribute. The smaller the entropy value, the larger is the entropy-based weight.

The entropy-weights for TL, MRR, RE and SR are 0.2632, 0.3421, 0.2342 and 0.1605, respectively. To verify the robustness of the entropy weights, this study conducted a sensitivity analysis using Monte Carlo simulations, performing 100 iterations with data perturbations ranging from 0% to 20%. The coefficients of variation for all quality characteristics were below 6% (Table 1), and the weight ranking remained unchanged, indicating excellent robustness. This study also constructed a Bootstrap 95% confidence interval, which was narrow (≤0.027), confirming its statistical reliability (Table 2). Error propagation analysis further indicated that the combined measurement uncertainty does not alter the primary optimization conclusion: MRR is the dominant criterion (weight = 0.3421 ± 0.0142), followed by TL (0.2632 ± 0.0089). An increase in MRR for TMM AISI 52100 bearing steel results in a significant decrease in the TL and RE, and increase in the SR of the workpiece. However, TMM quality is affected by the cutting conditions and cooling methods.

Table 1. Sensitivity analysis of quality characteristics using Monte Carlo simulation

Quality characteristic	Original Weight	Mean Weight (σ=5% noise)	Std. Dev.	CV (%)	Stability Rank
MRR	0.3421	0.3412	0.0142	4.2	Highly robust
TL	0.2632	0.2618	0.0089	3.4	Highly robust
RE	0.2342	0.2345	0.0113	4.8	Highly robust
SR	0.1605	0.1625	0.0098	6.0	Moderately robust

Table 2. Uncertainty analysis of quality characteristics via Bootstrap confidence intervals

Quality characteristic	95% Confidence Interval	Interval Width
MRR	[0.3284, 0.3558]	0.0274
TL	[0.2541, 0.2723]	0.0182
RE	[0.2225, 0.2469]	0.0244
SR	[0.1518, 0.1692]	0.0174

2.2 Desirability function analysis (DFA)

DFA is a commonly used multi-quality optimization statistical method that can convert multiple complex and conflicting thorny problems into a single, optimizable objective function and find the optimal solution. plan. Recently, several studies are reported on the application examples (product design, process optimization and material selection) of DFA in various fields. The steps for calculating DFA are as follows:

Step 1: Development of data matrix (X). Experiments were performed using Taguchi orthogonal array L9 to obtain the data matrix as shown in Eq. (1).

Step 2: Calculation of individual desirability function (d_i). Depending on the response characteristics, this desirability function has three different forms (a) nominally optimal (d_T), (b) larger is better (d_L), and (c) smaller is better (d_S). This study uses the "d_S" characteristic for the RE and SR output responses, and the "d_L" characteristic for the TL and MRR output responses. These d_L and d_S are shown in Eqs. (6)-(7).

$$d_L = \begin{cases} 0, & y_i \le y_{min} \\ \left(\frac{y_i - y_{min}}{y_{max} - y_{min}}\right)^r, & y_{min} \le y_i \le y_{max}, \quad r \ge 0 \\ 1, & y_i \ge y_{max} \end{cases} \tag{6}$$

$$d_S = \begin{cases} 0, & y_i \le y_{min} \\ \left(\frac{y_{max}-y_i}{y_{max}-y_{min}}\right)^r, & y_{min} \le y_i \le y_{max}, \quad r \ge 0 \\ 1, & y_i \ge y_{max} \end{cases} \tag{7}$$

where y_i is the response value, $y_{\min}$ is the lower tolerance limit, $y_{\max}$ is the upper tolerance limit and *r* is the weight.

Step 3: Calculation of composite desirability (d_G). All individual desirability of a reaction can be formed into a single value as the d_G using the Eq. (8).

$$d_G = \sqrt[n]{(d_1^{w1} \times d_2^{w2} \cdots d_i^{wi})} \tag{8}$$

where d_i and w_i are the individual desirability and weight of the individual attribute (E_i) and *n* is the number of the attribute. Thus, the value of d_G is capable of assessing the levels of the combined set of attributes and it varies from 0 to 1. The closest the value of d_G is to 1, the better is the optimization.

2.3 Grey relational analysis (GRA)

This study optimized the cutting process parameters and adopted the GRA, which has been widely used in various fields. The calculated steps for GRA are as follows:

Step 1: Development of data matrix (X) as shown in Eq. (1).

Step 2: Preprocess data matrix (*Y*) using the smaller-the-better and the larger-the-better criterions from Eqs. (9) and (10).

$$y_i = \frac{\max(x_i) - x_i}{\max(x_i) - \min(x_i)} \tag{9}$$

$$y_i = \frac{x_i - \min(x_i)}{\max(x_i) - \min(x_i)} \tag{10}$$

Step 3: Deviation sequence (D_S) of pre-processed data matrix.

$$D_S = 1 - y_i \tag{11}$$

Step 4: Calculation of grey correlation coefficient (GRC) [25].

$$\gamma_i = \frac{\min x_i + \xi \max x_i}{x_i + \xi \max x_i} \tag{12}$$

The differentiation coefficient value (ζ = 0~1) can be adjusted based on the actual system requirements. In this work, ζ is set to 0.5.

Step 5: Calculation of grey relational grade (ψ). It is defined as follows:

$$\psi = \sum_{i=1}^{n} w_i \times \psi_i \tag{13}$$

3. Experimental Procedure

3.1 Workpiece and experimental equipment

In this study, the workpiece was made of AISI 52100 HCRs (outer diameter of 25 mm, inner diameter of 18 mm, length of 528 mm, surface hardness of HRC 63, and inner layer hardness around of HRC 30). The experimental setup (Fig. 1) utilized a TMM (Chiah Chyun CB-36, Taiwan) and a tungsten carbide end mill (diameter of 6 mm, four cutting-edges) to mill a groove plane (depth of 1.5 mm, width of 10 mm). A vision measuring instrument (Nanjie Technology Co., Ltd. AF-3020, Taiwan) was used to observe the cutting-edge and analyze the milling cutter's service life. Fig. 2 shows the cutting-edge surface morphology of the cutter body at before cutting (new tool) and different stages after cutting (initial wear, cutting-edge cracks and cutting-edge damage). A SR meter (Hommel T1000 Wave) in Fig. 3 was employed to measure the SR of workpiece's after TMM AISI 52100 bearing steel (Fig. 4). In this study, a milling

cutter is considered seriously worn and needs to be replaced when Ra > 0.8 μm. The AISI 52100 HCR is precision ground with a RE of less than 0.01 mm. A V-shaped pillow is used to support the AISI 52100 HCR, and a lever micrometer is used to measure the RE (Fig. 5).

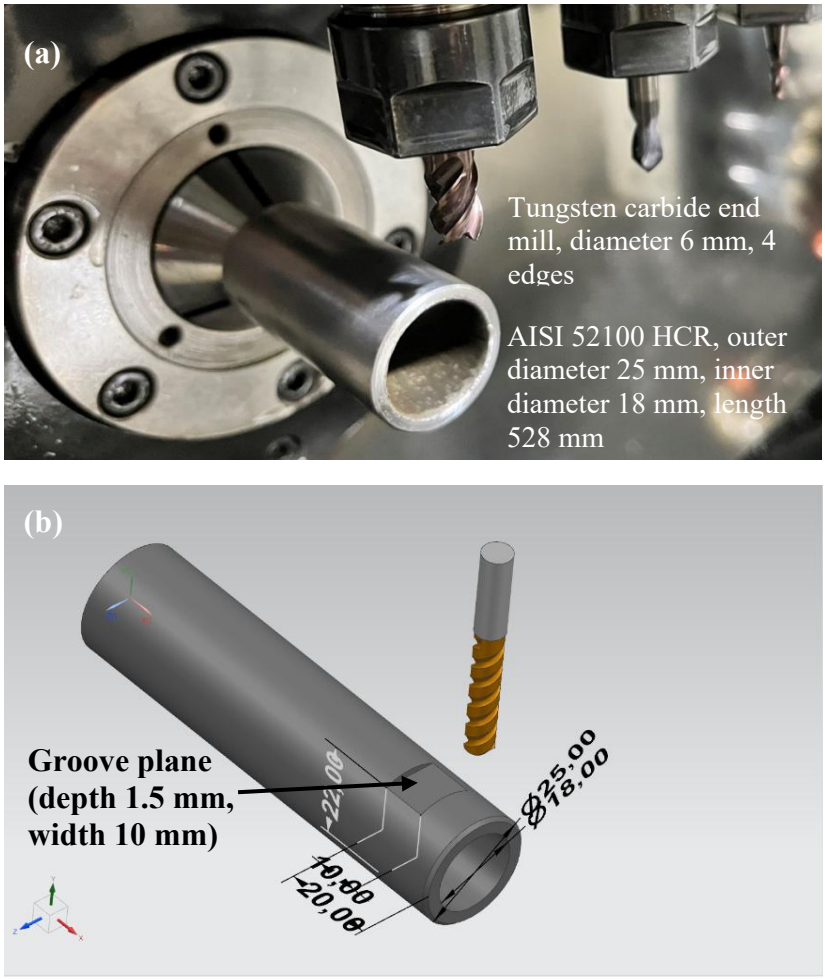


Fig. 1. (a) Experimental device and (b) groove depth of 1.5 mm × width of 10 mm) in TMM operation.

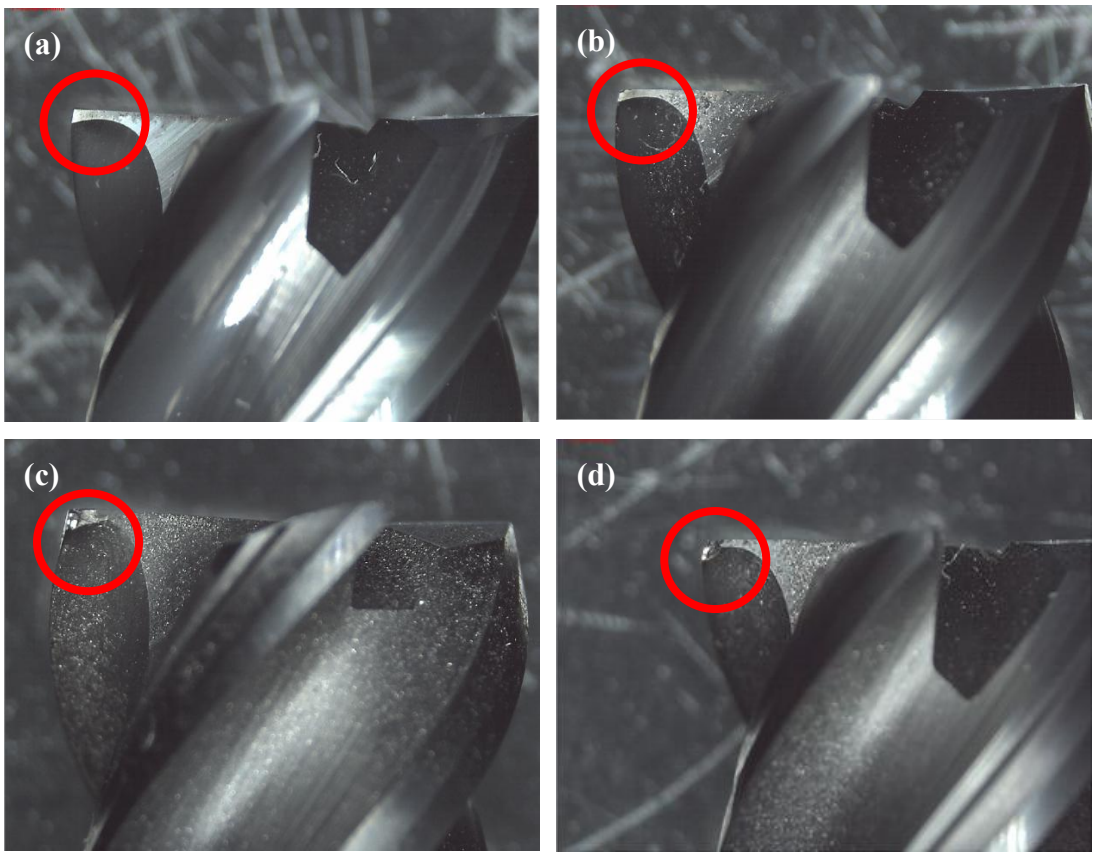


Fig. 2. Cutting-edge surface morphology, (a) new cutter (before cutting), (b) initial wear of cutter (after cutting), (c) cutting-edge cracks (after cutting), (d) cutting-edge breakage (after cutting).

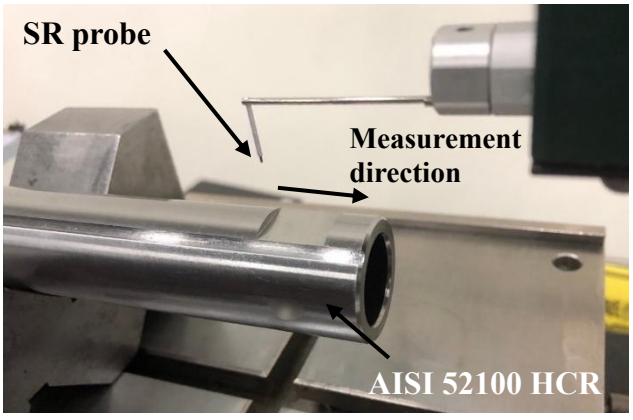
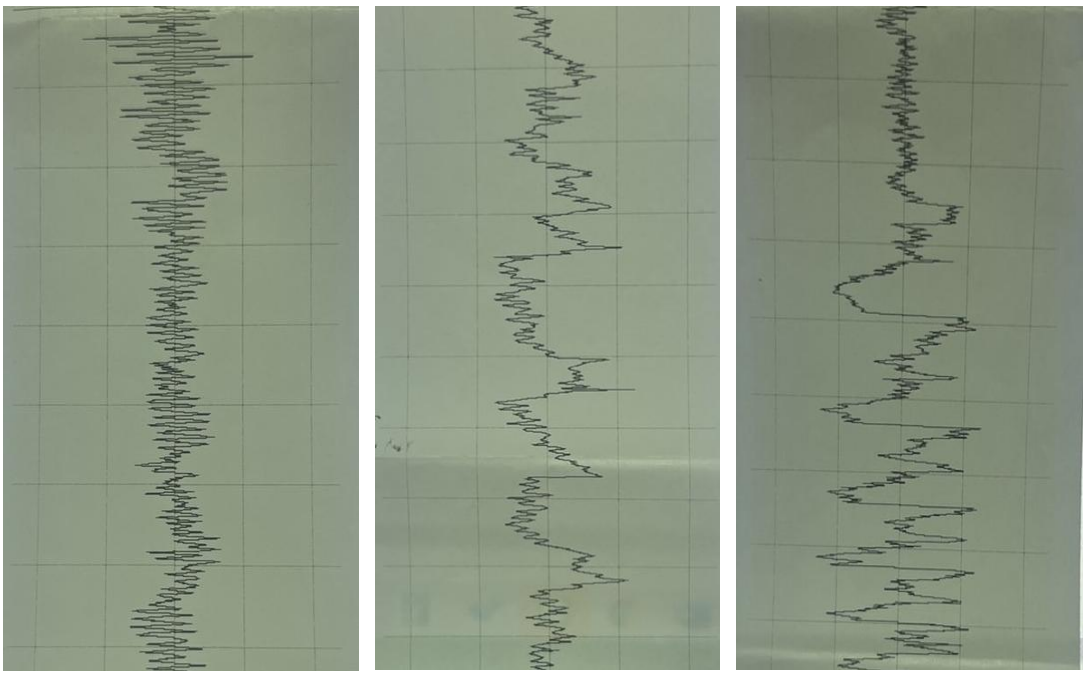


Fig. 3. SR measurement after TMM AISI 52100 bearing steel.



(a) Ra=0.218 µm (b) Ra=0.491 µm (c) Ra=0.527 µm

Fig. 4. SR of workpiece after TMM AISI 52100 bearing steel.

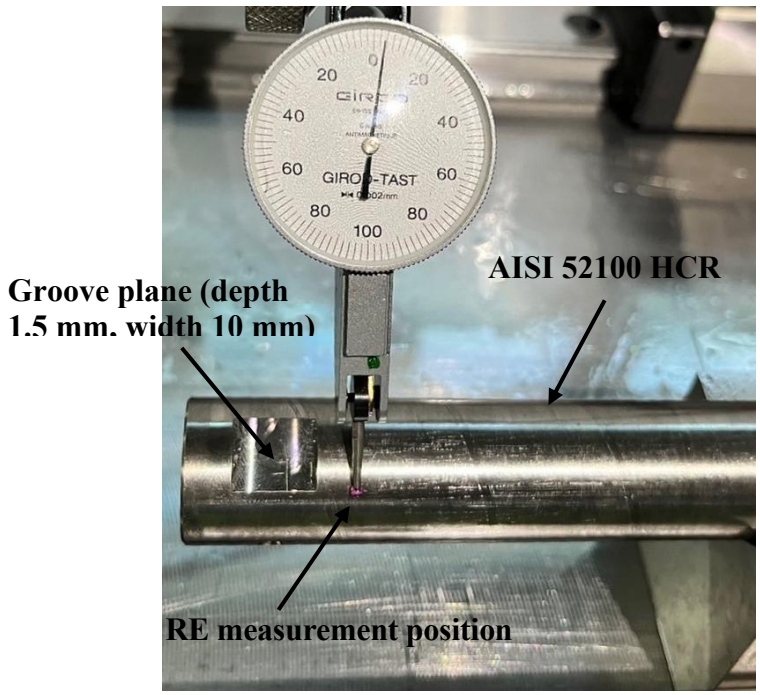


Fig. 5. Measuring the RE after TMM AISI 52100 HCRs.

3.2. Preliminary Cutting

To machine a groove on the outer diameter of the part, the TMCM spindle (C-axis) first rotates the workpiece to the groove angle and locks it in place. Then, the milling cutter on the PTH (radial) rotates. Subsequently, the tool feeds along the Z-axis or X-axis to mill a straight groove. Because the PTH can be indexed with the TMCM spindle (C-axis), it is very suitable for rotating parts that are primarily turned and secondarily milled, using process concentration to achieve overall machining efficiency and accuracy. However, its shortcomings of insufficient structural rigidity and spindle speed limitation become apparent when milling is performed under heavy loads, with high precision requirements, or when the material is difficult to cut.

Furthermore, the success or failure of finishing AISI 52100 bearing steel is directly affected by the appropriate selection of cutting tools and cutting parameters. Referring to the relevant literature [26], when the cutting speed is set to 110 m/min, cutting-edge breakage occurs (Fig. 6), indicating the need to reduce the cutting speed to 100m/min. At a cutting speed of 70m/min, the cutting process produces excessive noise and does not exhibit normal cutting status. Therefore, the cutting speeds in this study were set to 80, 90, and 100m/min, respectively. Feed rates are based on 0.5% of the milling cutter diameter (6 mm) and increase proportionally [26]. When the feed rate increases to 2% (0.12mm/rev), poor chip removal occurs, resulting in damage to the tool tip (Fig. 7 shows cutting-edge breakage), making it impossible to continue milling. Thus, this study adjusted the feed limit value to 1.5% of the milling cutter diameter (0.09mm/rev). Consequently, the feed rates were determined to be 0.03, 0.06, and 0.09mm/rev in the experiment. The outer diameter of the AISI 52100 HCR is $25^{-0.007}_{-0.02}$mm (tolerance g6). During the milling process of the groove plane, slight deformation may cause the rod to become defective (i.e., scrapped). When the cutting depth reached 0.8 mm, the study determined the rod to be defective due to excessive cutting load, resulting in cutting-

edge cracks and RE exceeding 0.05 mm. Therefore, the adjusted cutting depths were set to 0.1, 0.25, and 0.5 mm, respectively. Additionally, the study compared three cooling modes: air cooling, emulsified oil, and oil mist cooling. Taguchi's experimental design (L_9) was employed to optimize the cutting process. This experiment selected four cutting parameters - cutting speed, feed rate, cutting depth, and cooling method - each assigned high, medium, and low levels. Table 3 lists the cutting parameters, factors, and levels. This study examines the effect of each cutting parameter on TL, MRR, RE, and SR.

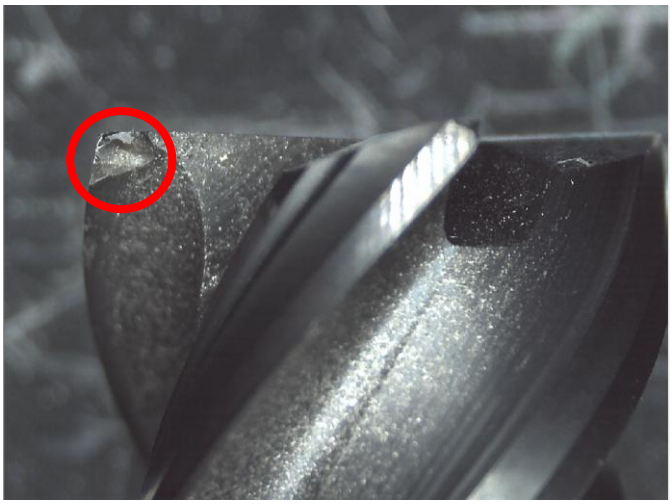


Fig. 6. Cutting-edge breakage, using cutting speed is 110 m/min.

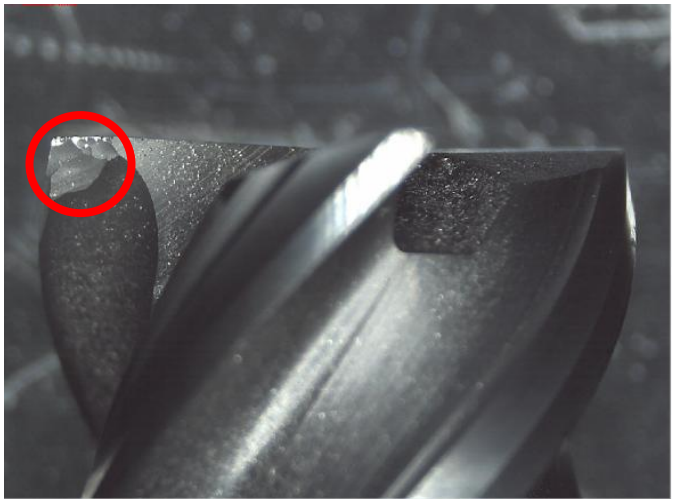


Fig. 7. Cutting-edge breakage, using feed rate is 0.12 mm/rev.

Table 3. Cutting parameters, factors and levels.

Turn-milling compound CNC		Chiah Chyun CB-36		
Tungsten carbide end mill		Diameter 6 mm, four cutting-edges (G-TOP)		
Workpiece material		AISI 52100 HCRs		
Workpiece dimension		25 mm (outer)×18 mm (inner)×528 mm		
Milling dimensions		10 mm (width) ×1.5 mm (depth)		
Symbol	Control factor	Level 1	Level 2	Level 3
A	Cutting speed (m/min)	80	90	100
B	Feed rate (mm/rev)	0.03	0.06	0.09
C	Cutting depth (mm)	0.10	0.25	0.50
D	Cooling method	Air	Emulsified oil	Oil mist

4. Results and Discussion

4.1 Taguchi design for cutting processing

According to Taguchi's experimental design (L_9), each milling parameter set was repeated three times. In this study, TL and MRR are considered "higher is better" (HB) performance characteristics, while RE and SR are "lower is better" (LB). The arc volume of the milled double-sided groove plane (groove depth of 1.5 mm, groove width of 10 mm, outer diameter of 25 mm) is estimated to be 428 mm^3. The tool has completed milling the double-sided groove plane (volume is 428 mm^3). The TL is defined as one piece if the cutting-edge is not broken; if the cutting-edge breaks, the tool's life is considered terminated.

Table 4 lists the experimental design matrix with response values. To evaluate the relative impact of cutting parameters on the measurement responses, an analysis of variance (ANOVA) was performed at a 95% confidence level. The results for TL, MRR, RE, and SR showed that C and D both had statistically significant effects, while B had a significant impact on SR (Table 5). The most dominant cutting parameter was D, accounting for 92.96%, 86.41%, 96.44%, and 91.46% of the total variance in TL, MRR, RE, and SR, respectively. The coefficient of determination (R^2) serves multiple

important purposes in ANOVA and regression analyses. Fig. 8 compares the four responses with R^2 and adjusted R^2. In this study, the R^2 of all four responses is greater than 90%, indicating that the Taguchi L_9 array experimental design (factor selection and level range setting) is good, and its measurement error is small (residual variation is less than 4%). These results suggest that D is the dominant factor, and better cutting lubrication helps to reduce the shearing effect of the tool on the workpiece and improve surface finish.

Table 4. Experimental design matrix with response values.

No.	Factors A B C D	TL (pieces)	MRR (mm^3/sec)	RE (mm)	SR (Ra)
1	1 1 1 1	1.67	1.51	0.043	0.669
2	1 2 2 2	24.33	52.60	0.012	0.243
3	1 3 3 3	6.67	36.58	0.028	0.542
4	2 1 2 3	8.33	17.31	0.024	0.464
5	2 2 3 1	1.00	5.10	0.051	0.857
6	2 3 1 2	27.00	46.14	0.010	0.238
7	3 1 3 2	17.33	69.10	0.015	0.284
8	3 2 1 3	10.00	9.39	0.022	0.274
9	3 3 2 1	1.33	3.04	0.045	0.827

Table 5. ANOVA results and the contribution ratio of important cutting parameters, which corresponds to Table 4.

Factor	Degree of freedom	Sum of square	Variance	F-ratio	Contribution ratio (P %)
TL (R^2=96.99%, R^2_{adj}=93.97%)					
C	2	32.22	16.11	2.84	4.13
D	2	726.00	363.00	63.91	92.96
Pooling error	4	22.72	5.68		2.91
Total	8	780.94			100.00
MRR (R^2=96.79%, R^2_{adj}=93.58%)					
C	2	508.35	254.175	5.97	10.18
D	2	4315.38	2157.69	50.70	86.41
Pooling error	4	170.22	42.555		3.41
Total	8	4993.95			100.00
RE (R^2=99.82%, R^2_{adj}=99.63%)					
C	2	0.00006219	3.11E-05	36.80	3.37

D	2	0.00177750	0.000889	1051.78	96.44
Pooling error	4	0.00000338	8.45E-07		0.18
Total	8	0.00184307			100.00
SR (R^2=98.97%, R^2_{adj}=95.88%)					
B	2	0.01038	0.00519	2.03	2.09
C	2	0.04408	0.02204	8.61	8.88
D	2	0.43688	0.21844	85.33	88.00
Pooling error	2	0.00512	0.00256		1.03
Total	8	0.49646			100.00

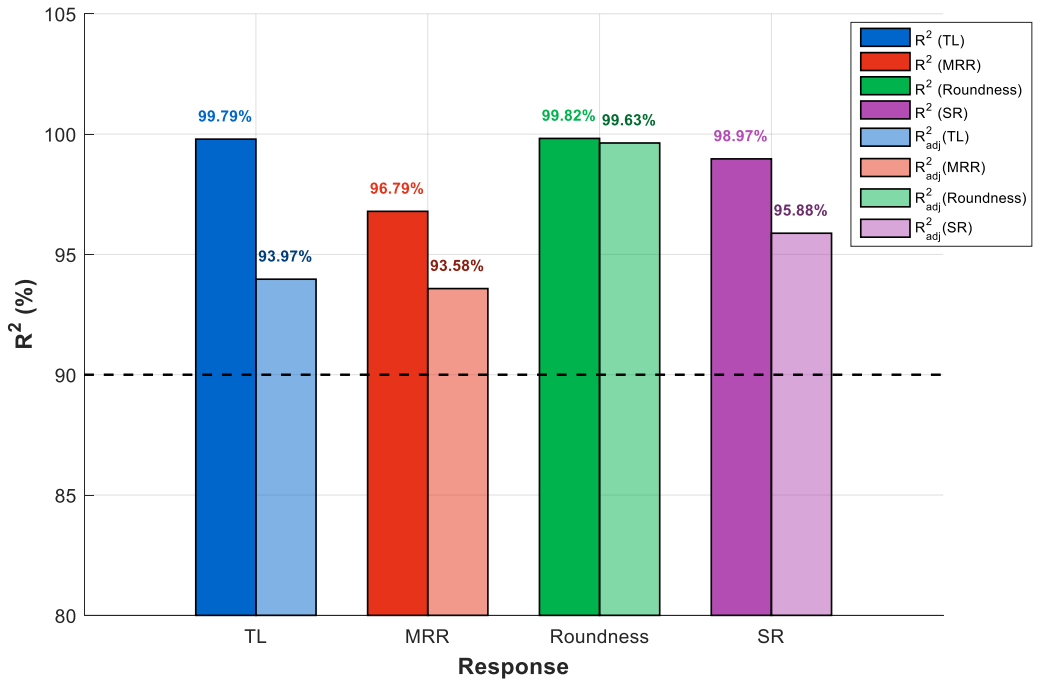


Fig. 8. Comparison of four responses with R² and adjusted R²

Table 6 shows the results for the DFA and GRA, which gives an almost complete ranking for the TMM configurations. Table 6 shows that using the DFA, the experiment of No. 6 TMM combination ($A_2B_3C_1D_2$) has the most d_G and the highest rank for the overall TMM configurations, which is almost same as the GRA result. High-speed cutting (90 m/min) combined with high feed (0.09 mm/rev) and shallow depth of cut

(0.10 mm), under emulsion oil cooling, can effectively reduce cutting temperature, reduce tool wear, and improve the surface quality of the machined parts, thus achieving the best balance in MQCs. Although DFA can be used more simply than the GRA to determine the MQC of engineering problems. However, when the d_i of a certain quality characteristic is 0 (Nos. 1 and 5), the d_G is also 0. This result will affect the subsequent ANOVA calculation and the search for the global optimal parameter combination. Therefore, this study uses the GRA for subsequent ANOVA calculations and the search for the global optimal parameter combination.

Table 6. Results for the DFA and for GRA.

No.	d_G	Rank for DFA	ψ	Rank for GRA
1	0.0000	8	0.3584	7
2	0.9663	1	0.8178	3
3	0.8047	4	0.4807	5
4	0.7786	5	0.4732	6
5	0.0000	8	0.3358	9
6	0.9651	2	0.8597	1
7	0.9595	3	0.8210	2
8	0.7586	6	0.5274	4
9	0.4294	7	0.3443	8

Table 7 presents the ANOVA results for GRA on ψ. From Table 7, the cooling method has the most significant effect on ψ (P = 98.86%). Emulsified oil cooling produces the best cutting results. In TMM, the cooling method significantly impacts the combined effects of heat, friction, adhesion, and tool life. Because emulsified oils effectively remove cutting heat and provide excellent lubrication, they reduce built-up

edge formation, lower temperature and friction during TMM, thereby extending tool life and improving workpiece surface quality. These characteristics are directly reflected in the multiple quality indicators integrated by GRA, making emulsified oils a key factor determining overall machining quality. Although the relatively optimal cutting parameters for cutting speed, feed rate and depth of cut for AISI 52100 bearing steel were determined through preliminary cutting (Section 3.2), their effects were not significant. During hard cutting of AISI 52100 bearing steel, intense thermo-mechanical action may form a thin, altered white layer on its surface, necessitating optimization of cutting parameters to control cutting heat generation [27, 28]. TL and MRR increase with the use of moderate feed speeds and emulsified oil cooling. The SR is lower at higher cutting speeds, medium feeds, and lower cutting depth. RE increases with decreasing feed rate and cutting depth and with the use of emulsified oil cooling. However, using appropriate cooling methods (emulsified oil) can increase cutting speed and MRR.

Table 7. The ANOVA results for GRA on ψ.

Factor	Level 1	Level 2	Level 3	Degree of freedom	Sum of square	Variance	Contribution (P %)
A	0.5581	0.5644	0.5683	2	0.0002	0.0001	0.04
B	0.5538	0.5687	0.5684	2	0.0004	0.0002	0.11
C	0.5924	0.5524	0.5461	2	0.0038	0.0019	0.99
D	0.3488	0.8397	0.5024	2	0.3783	0.1892	98.86
Total				8	0.3827		100

4.2. Optimize cutting parameters

The GRA can solve complex inter-relationships among multiple characteristics [13]. The optimization of the grey correlation grade (GRG) and its ranking in the cutting

process, as calculated using Eqs. (12) and (13), are presented in Table 6. A higher GRG indicates that the experimental results are closer to the ideal normalized value. The parameter set (No. 6, $A_2B_3C_1D_2$: cutting speed of 90 m/min, feed rate of 0.09 mm/rev, cutting depth of 0.10 mm, and emulsified oil cooling method) exhibits the optimal performance characteristics of the nine experiments.

Table 7 provides the ANOVA results for MQCs during the cutting process, with the optimal combination being $A_3B_2C_1D_2$: cutting speed of 100 m/min, feed rate of 0.06 mm/rev, cutting depth of 0.10 mm, and emulsified oil cooling method. To confirm the reliability of the TMM AISI52100 HCR, this study repeated the experiment three times using the optimal milling parameters ($A_3B_2C_1D_2$). Table 8 compares the quality characteristics of the optimal milling parameters ($A_3B_2C_1D_2$) with those of No. 6 ($A_2B_3C_1D_2$) in Table 6, revealing improvements of 22.22% in TL, 16.45% in material removal rate, 10.00% in RE, and 8.40% in SR.

Table 8. Comparing the quality characteristics of optimal milling parameters ($A_3B_2C_1D_2$) with No. 6 in Table 4 ($A_2B_3C_1D_2$).

Quality characteristic	Orthogonal array $A_2B_3C_1D_2$ (No.6)	Optimal parameters $A_3B_2C_1D_2$	Improvement rate (%)
TL (pieces) HB	27	33	22.22
MRR (mm^3/sec) HB	26.14	30.44	16.45
RE (mm) LB	0.010	0.009	10.00
SR (Ra, μm) LB	0.238	0.218	8.40

4. Conclusion

This paper presents the experimental investigation and multi-quality optimizations of TMM of AISI 52100 bearing steels by the DFA and GRA. From the results of

optimization and ANOVA, the following conclusions are drawn.

(1) The analysis of ranking by adopting DFA and GRA indicated the experiment of No. 6 (cutting speed of 90 m/min, feed rate of 0.09 mm/rev, cutting depth of 0.10 mm, and emulsified oil cooling method, $A_2B_3C_1D_2$). However, when using DFA to calculate d_G, it is easy for a certain quality characteristic value to be 0, resulting in inaccuracy in subsequent ANOVA.

(2) The ANOVA for GRA on ψ reveals that cooling method (emulsified oil) is the main TMM parameter, which has a higher effect on the process quality (P = 98.86%).

(3) The optimal cutting conditions for GRA on ψ are cutting speed of 100 m/min, feed rate of 0.06 mm/rev, cutting depth of 0.100 mm, and emulsified oil cooling method ($A_3B_2C_1D_2$).

(4) In the confirmation experiment, the quality characteristics of the optimal milling parameters ($A_3B_2C_1D_2$) and No. 6 ($A_2B_3C_1D_2$) in Table 5 were compared. The TL, MRR, RE and SR were increased by 22.22%, 16.45%, 10.00% and 8.40%, respectively.

Declarations

Conflict of interest The authors state no conflict of interest.

Ethics approval Not applicable.

Consent to participate Not applicable.

Consent for publication Not applicable.

Data availability Not applicable.

Acknowledgments

The authors gratefully acknowledge the support of the National Science and Technology Council, Taiwan (ROC) through Grant Nos. NSTC 115-2622-E-262-003 and NSTC 115-2637-E-262-001.

References

1. Li P, Zhao R, Luo L (2020) A geometric accuracy error analysis method for turn-milling combined NC machine tool. Symmetry 12:1622-1639. https://doi.org/10.3390/sym12101622
2. Zheng, ZP, Jin X, Sun YW, Zhang ZJ, Sun HC, Li QM (2020) Prediction of chatter stability for enhanced productivity in parallel orthogonal turn-milling. Int. J. Adv. Manuf. Technol. 110:2377-2388. https://doi.org/10.1007/s00170-020-06015-0
3. https://www.jshfcnc.com/news/749.html, 2026.
4. Karaguzel U, Uysal E, Budak E, Bakkal M (2016) Effects of tool axis offset in turn-milling process. J. Mater. Process. Technol. 231:239-247. http://dx.doi.org/10.1016/j.jmatprotec.2015.12.020
5. Liao Z, Axinte D, Gao D (2019) On modelling of cutting force and temperature in bone milling. J. Mater. Process. Technol. 266:627-638. 10.1016/j.jmatprotec.2018.11.039
6. Cai Y, Ma Y, Chao H, Yao X (2015) Swept area modeling and cutter wear study in turn-milling. Int. J. Adv. Manuf. Technol. 80:775-789. https://doi.org/10.1007/s00170-015-7021-6
7. Zhu L, Jin X, Liu C (2016) Experimental investigation on 3D chip morphology properties of rotary surface during orthogonal turn-milling of aluminum alloy. Int. J. Adv. Manuf. Technol. 84:1253-1268. https://doi.org/10.1007/s00170-015-7758-y

8. Ning JS, Zhu LD (2019) Parametric design and surface topography analysis of turbine blade processing by turn-milling based on CAM. Int. J. Adv. Manuf. Technol. 104:3977-3990. https://doi.org/10.1007/s00170-019-04037-x

9. Vijayakumar R, Pannirselvam N (2022) Employing desirability function analysis for the multi-response optimisation of mild steel embossed plate shear connector using Taguchi technique. Sustain. Energy Technol. Assess. 54:102863-102872. 10.1016/j.seta.2022.102863

10. Allah MMA, El-baky MAA (2024) Multi-objective optimization through desirability function analysis on the crashworthiness performance of thermoplastic/thermoset hybrid structures. Compos. Pt. B-Eng. 284:111742-111754. https://doi.org/10.1016/j.compositesb.2024.111742

11. Parameshwara S, Girisha KB, Pradeep NB, Manjunath Patel GC, Emanoil L, Manjunath SH (2025) Integrated optimization of mechanical alloying parameters for nanostructured Ti-Mg-Zr alloy using desirability function, educational competition. and grey wolf algorithms. Results Eng. 26:104748-104766. https://doi.org/10.1016/j.rineng.2025.104748

12. Sahare S, Kamble P, Giri J, Sunheriya N, Sathish T, Chadge R, Parthiban A (2024) Multi objective optimization of cutting parameters of end milling operation by Taguchi Grey Relational analysis (TGRA). Interactions 245:273291. https://doi.org/10.1007/s10751-024-02119-1

13. Suvvari SGP, Kandru S, Chappa M (2024) Optimization of cement, rice husk ash, and waste plastic additives for stabilizing expansive subgrade soil: a Grey-Taguchi analysis approach. J. Build. Pathol. Rehabil. 9:8-18. https://doi.org/10.1007/s41024-023-00357-4

14. Ravindrannair P, Equbal A, Equbal MA, Saxena KK, Equbal MI (2024) Grey based

Taguchi method for multi-response optimization of FSW of aluminium AA 6061 alloy. Int. J. Interact. Des. Manuf. 18:1279-1290. https://doi.org/10.1007/s12008-023-01557-5

15. Jin CZ, Fang R (2014) Research on surface topography and roughness of micro parts by high speed turn-milling. Mater. Sci. Forum 800-801:607-612.
16. Ekici E, Uzun G (2022) Effects on machinability of cryogenic treatment applied to carbide tools in the milling of Ti6AI4V with optimization via the Taguchi method and grey relational analysis. J. Braz. Soc. Mech. Sci. Eng. 44(7):270-283. https://doi.org/10.1007/s40430-022-03572-1
17. Sghaier TAM, Sahlaoui H, Mabrouki T, Sallem H, Yallese MA, Rech J (2026) Multi-response optimization of turning parameters for laser powder bed fusion 17-4PH stainless steel using PCA-GRA. Int. J. Mater. Form. 19:79. https://link.springer.com/article/10.1007/s12289-026-02047-1
18. Jattakul P, Mhoraksa T, Kanlayasiri K (2024) Optimization of the Solid-State Copper Brazing Condition Using Desirability Function and Genetic Algorithm. Arab. J. Sci. Eng. 49:14729-14739. https://doi.org/10.1007/s13369-024-08791-3
19. Cardoso LG, Madeira DS, Ricomini TEPA, Miranda RA, Brito TG, Paiva EJ (2021) Optimization of machining parameters using response surface methodology with desirability function in turning duplex stainless steel UNS S32760. Int. J. Adv. Manuf. Technol. 117:1633-1644. https://doi.org/10.1007/s00170-021-07690-3
20. Lu SQ, Chiu LH (2024) Effect of different microstructures on surface residual stress of induction-hardened bearing steel. Metals 14(2): 201-212. https://doi.org/10.3390/met14020201
21. Widmaier T, Hemming B, Juhanko J, Kuosmanen P, Esala VP, Lassila A, Laukkanen P, Haikio J (2017) Application of Monte Carlo simulation for estimation of

uncertainty of four-point roundness measurements of rolls. Precis. Eng. 48:181-190. http://dx.doi.org/10.1016/j.precisioneng.2016.12.001

22. Chen KT, Hu CC, Hsu CY, Tsao CC, Hong PD (2020) Optimizing the multi-attribute characteristics (MACs) of CrWN hard film tool in turning AISI 304 stainless steel. J. Mater. Eng. Perform. 29:2506-2513. https://doi.org/10.1007/s11665-020-04732-x

23. Dubey AK, Kumar Y, Kumar S (2025) Optimizing parameters of AWJM for Ti-6Al-4 V grade 5 alloy using grey entropy weight method: a multivariable approach. J. Inst. Eng. India Ser. C, 106(1):181-195. https://doi.org/10.1007/s40032-024-01139-8

24. Ozdogan AK, Varol MK, Demirdag S (2026) Determination of cutting performance of multi-blade and diamond-wire gang saws used in natural stone cutting. Mining Metall. Explor. 43:2121-2139. https://doi.org/10.1007/s42461-026-01540-0

25. Deng JL (1989) Introduction to Grey system. J. Grey Syst. 1:1.

26. Liu M, Takagi JI, Tsukuda A (2004) Effect of tool nose radius and tool wear on residual stress distribution in hard turning of bearing steel. J. Mater. Process. Technol. 150(3):234-241. doi:10.1016/j.jmatprotec.2004.02.038

27. Kokkirala S, Osman K, Holmberg J, Kimming S, Iwasaki H, Klement U, Hosseini SB (2024) The role of retained austenite on the formation of the nanostructured hard-turned induced white layer in AISI 52100 bearing steel. Procedia CIRP 123:292-297. https://doi.org/10.1016/j.procir.2024.05.052

28. Rajbongshi SK, Sarma D K, Singh MA (2020) A brief review of white layer formation in hard machining with a case study. Adv. Mech. Eng. 407-417. https://doi.org/10.1007/978-981-15-0124-1_36

Supplementary Files

This is a list of supplementary files associated with this preprint. Click to download.

- Highlights.docx